

Multiwavelength Polarization as a Diagnostic of Blazar Physics

Markus Böttcher^{*†}

Centre for Space Research, North-West University, Potchefstroom, 2520, South Africa
E-mail: Markus.Bottcher@nwu.ac.za

Haocheng Zhang

Theoretical Division, Los Alamos National Laboratory, Los Alamos, NM 87545, USA
E-mail: phitlip2007@gmail.com

Xuhui Chen

DESY, Platanenallee 6, D-15738 Zeuthen, Germany
Institute for Physics and Astronomy, University of Potsdam, D-14476 Potsdam-Golm, Germany
E-mail: chenxuhui.phys@gmail.com

The nature of the high-energy emission in jet-dominated AGN (especially blazars) as well as the location and mode of acceleration of particles to ultra-relativistic energies are a matter of intensive debate. Both leptonic and hadronic origins of the high-energy emission are still possible, and spectral energy distribution (SED) modeling alone is not sufficient to distinguish between leptonic and hadronic models. We will discuss high-energy (X-ray and γ -ray) polarization as a possible diagnostic to distinguish leptonic from hadronic models, showing that substantial X-ray and gamma-ray polarization would be a tell-tale signature of hadronic high-energy emission. Motivated by these results, the potential impact of γ -ray polarization on the evaluation of $\gamma\gamma$ absorption of high-energy γ -rays from relativistic jets will be discussed. Finally, we turn to the occasionally observed feature of large ($\geq 180^\circ$) swings of the optical polarization angle correlated with multi-wavelength flaring activity in several blazars. We suggest an interpretation not requiring any helical pattern motions or bent jets, simply based on a helical magnetic field pervading a straight jet. We present simultaneous fits to the SEDs, multi-wavelength light curves and time-dependent optical polarization features (degree and angle) in one coherent model for the prominent polarization-angle swing + γ -ray flaring event observed in 3C279. Such an interpretation requires a mode of conversion of magnetic energy to particle energy (e.g., magnetic reconnection) as the driving mechanism of such flaring activity.

*3rd Annual Conference on High Energy Astrophysics in Southern Africa ,
18-20 June 2015
University of Johannesburg, Auckland Park, South Africa*

^{*}Speaker.

[†]The work of M. B. is supported through the South African Research Chair Initiative (SARChI) of the South African National Research Foundation (NRF) and the Department of Science and Technology, under SARChI Chair grant no. 64789. *Disclaimer:* Any opinion, finding and conclusion or recommendation expressed in this material is that of the authors and the NRF does not accept any liability in this regard.

1. Introduction

Blazars are a class of radio-loud active galactic nuclei (AGN) whose multi-wavelength emission is strongly dominated by non-thermal emission emanating from a relativistic jet pointing at a small angle with respect to our line of sight. The spectral energy distributions (SEDs) of blazars consist of two broad non-thermal radiation components. The low-energy (radio through optical – UV, but in some cases extending into the X-ray regime) radiation is well understood as synchrotron emission from relativistic electrons in the jet, while the origin of the high-energy (X-ray through γ -ray) emission is still under debate. Both leptonic models and hadronic models are often equally well able to reproduce the SEDs of blazars (see, e.g., [5]). In leptonic models, the high-energy emission is produced by Compton up-scattering of synchrotron (SSC = synchrotron self-Compton) or external (EC = external Compton radiation) soft photons. In hadronic models, the high-energy emission is due to synchrotron radiation from ultrarelativistic protons and/or decay products of photopion production by ultrarelativistic protons and subsequent electromagnetic cascades. However, it has been pointed out in [23] that hadronic models tend to require extreme jet powers which appear to be in contradiction with our current understanding of jet launching by the Blandford-Znajek [3] or the Blandford-Payne [4] mechanisms.

In a search for possible diagnostics to distinguish between a leptonic and a hadronic origin of the X-ray and γ -ray emission from blazars, Zhang & Böttcher [24] have evaluated the high-energy polarization signatures from both types of models, and found that only hadronic models are expected to lead to potentially measurable degrees of γ -ray polarization. These results are briefly summarized below in Section 2. Motivated by the results of [24] that γ -rays produced in relativistic jet sources (in particular, radio-loud AGN and gamma-ray bursts) maybe highly polarized, [6] considered, for the first time, the possible impact of γ -ray and target-photon polarization on the absorption of high-energy γ -rays by the pair production process, $\gamma\gamma \rightarrow e^+e^-$. The results of that study will be summarized in Section 3.

In contrast to high-energy polarization in blazars, which has, so far, not been detected observationally, the (most likely synchrotron) radio and optical emission of blazars is well known to be often highly (up to $\sim 40\%$) polarized. Most intriguingly, the optical polarization angle of blazars has been observed to undergo large-angle ($\geq 180^\circ$) swings in tandem with multi-wavelength flaring activity (e.g., [17, 18, 1]). While such events have previously been interpreted as the signatures of helical pattern motions and/or bent jets, Zhang et al. [25, 26] have shown that a helical magnetic field pervading a straight jet naturally produces such polarization-angle swings when carefully accounting for light-travel time effects. In Section 4 we summarize the results of Zhang et al. [25, 26] who developed the first coherent, time-dependent model that is capable of reproducing simultaneously snap-shot SEDs, multi-wavelength light curves, and time-dependent polarization features (degree and angle).

2. X-ray and γ -ray Polarization

While the measurement of radio and optical polarization from blazars is commonly performed in many multiwavelength or dedicated optical polarization monitoring programs, X-ray and γ -ray polarization is still in its infancy. However, there are several on-going developments of X-ray

polarimeters, with several projects proposed for NASA’s SMEX program and significant developments in Europe and India, and γ -ray polarimetry may be feasible in pair conversion telescopes (such as Fermi-LAT or the envisioned PANGU detector [10, 22]) in the near future. Hence, there is interest in theoretical predictions of the X-ray and γ -ray polarization from blazars.

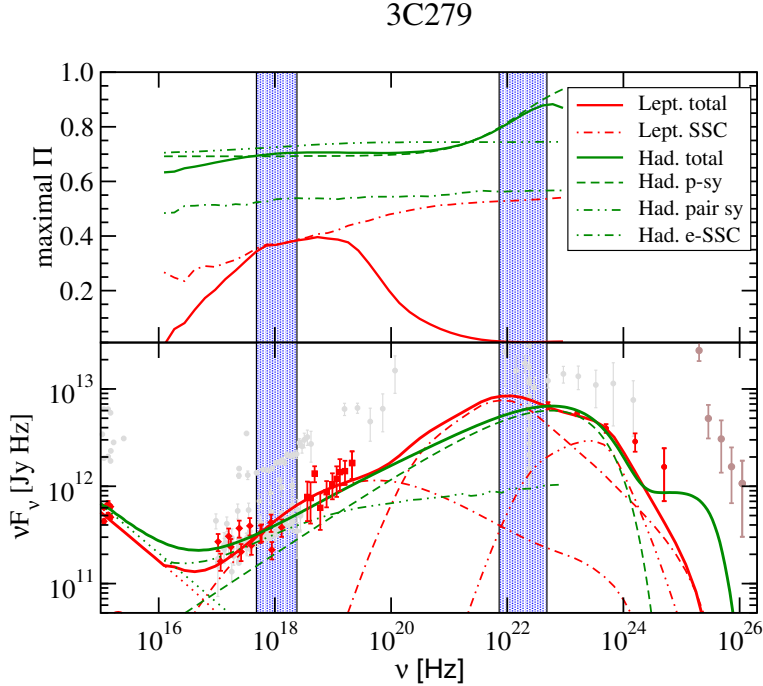


Figure 1: UV through γ -ray SEDs (lower panels) and maximum degree of polarization (upper panels) for the FSRQ 3C279. Leptonic model fits are plotted in red, hadronic models in green. Different line styles indicate individual radiation components, as labeled in the legend. Shaded areas indicate the 2 – 10 keV X-ray range (X-ray polarimeters) and the 30 – 200 MeV range, in which γ -ray emission may be measurable by *Fermi*-LAT. Grey data points are archival data which have not been included in the fit.

Zhang & Böttcher [24] have evaluated the multi-wavelength (including X-ray and γ -ray) polarization signatures from both leptonic and hadronic models of blazars. They started out with the SED fits to a number of Fermi-LAT detected blazars presented in [5]. Upper limits on the expected degree of polarization were calculated by assuming a perfectly ordered magnetic field oriented perpendicular to the line of sight to the high-energy emission region. For this purpose, the standard formalism for synchrotron polarization as presented in [21] has been used. The frequency-dependent degree of polarization of SSC emission has been evaluated using the expressions in [7, 8] for Compton scattering in the Thomson regime, which has been shown to be a valid assumption in the relevant energy regime of $E \lesssim 1$ GeV. Due to the approximate axisymmetry, EC emission has been assumed to be unpolarized.

Figure 1 shows the results for the blazar 3C279 as an example. The lower panel shows a zoom-in on the UV to γ -ray portion of the SEDs, with both a leptonic (red) and hadronic (green) model fit from [5]. The upper panel presents the predicted maximum degree of polarization. These upper limits may be converted into realistic estimates of the degree of polarization when considering the actually observed optical degree of polarization: An upper limit on the optical synchrotron

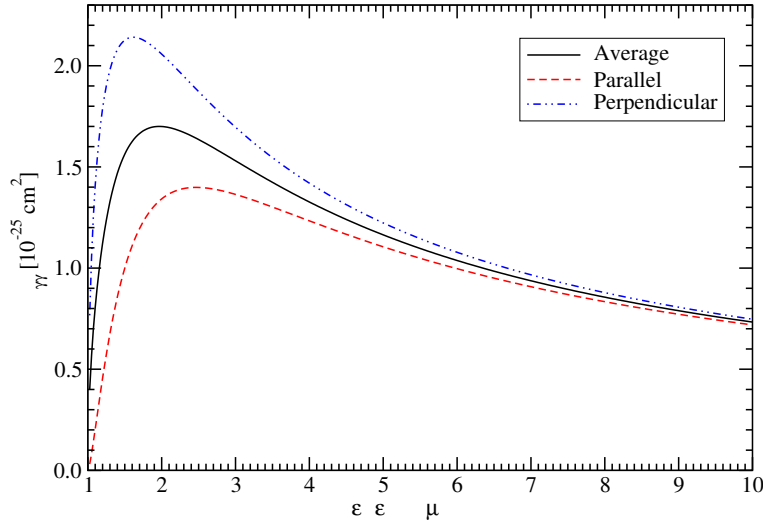


Figure 2: Polarization-dependent $\gamma\gamma$ absorption cross section as a function of center-of-momentum electron energy squared, $\gamma_{\text{cm}}^2 = \varepsilon_\gamma \varepsilon_t (1 - \mu)/2$, for the case of parallel and perpendicular polarization directions of γ -ray and target photons, respectively.

polarization, corresponding to a perfectly ordered magnetic field, can be inferred from the observed optical (synchrotron) spectral index through $\Pi_{\text{max}} = (\alpha + 1)/(\alpha + 5/3)$. Comparing this value to the actually observed degree of polarization yields a correction factor (typically about 0.2 — 0.4) accounting for the degree of dis-order of the magnetic field, by which the curves in the upper panels of Figure 1 should be multiplied to obtain a realistic prediction of the expected degree of polarization.

This example illustrates that hadronic models predict a potentially measurable level of X-ray and γ -ray polarization of $\sim 10 - 20\%$, while leptonic models do not. This conclusion holds in particular for low-frequency peaked blazars, while the X-ray emission from high-frequency peaked blazars is often dominated by synchrotron emission from primary electrons in both leptonic and hadronic models, thus predicting identical degrees of X-ray polarization. However, even in high-frequency peaked blazars, a potentially measurable degree of γ -ray polarization is only expected from hadronic models. A caveat that needs to be pointed out here is the underlying assumption that the optical (synchrotron) emission originates from the same region as the high-energy emission, or at least that the degree of ordering of the magnetic field is identical in the optical and γ -ray emitting regions.

3. $\gamma\gamma$ Absorption of Polarized γ -rays

High-energy γ -rays of energy ε_γ (normalized to the electron rest mass energy, $\varepsilon_\gamma = E_\gamma/m_e c^2$) may be absorbed by lower-energy target photons (normalized energy ε_t) through the process of $\gamma\gamma$ pair production, if the energies exceed the threshold condition $\varepsilon_\gamma \varepsilon_t (1 - \mu) \geq 2$ (where μ is the cosine of the interaction angle). This process may be important in high-compactness (i.e., very luminous, very small) γ -ray sources, such as the high-energy emission regions of blazars or

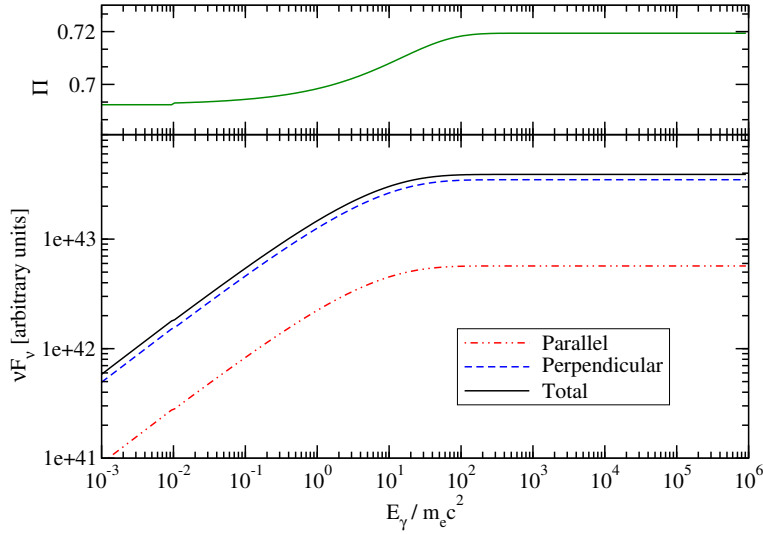


Figure 3: Polarization-dependent flux spectrum (lower panel) and degree of polarization as a function of photon energy (upper panel), in a synchrotron-dominated source with compactness $\ell = 1$ and synchrotron spectral index $\alpha = 0.5$.

gamma-ray bursts (GRBs), and the apparent absence of spectral signatures of $\gamma\gamma$ absorption has been used to infer lower limits on the Doppler factor of the bulk motion of the emission regions in blazars and GRBs [13, 2].

In all previous considerations of $\gamma\gamma$ absorption in astrophysical contexts, effects of polarization (of high-energy and target photons) have been ignored, using the polarization-averaged cross section for $\gamma\gamma$ absorption. However, the results presented in the previous section motivated us [6] to investigate the polarization-dependence of $\gamma\gamma$ absorption. The expression for the polarization-dependent $\gamma\gamma$ cross section can be found in [9, 6], and the resulting energy dependence for the two cases of parallel and perpendicular polarization directions of the γ -ray and target photons are plotted in Figure 2, compared to the polarization-averaged cross section.

Figure 2 illustrates that the $\gamma\gamma$ absorption of polarized γ -ray photons is preferred (with about a factor 1.5 larger peak cross section) for the interaction with target photons of polarization angles perpendicular to the γ -ray photon, while it is correspondingly suppressed for the interaction with target photons of identical polarization angle. The latter is expected to be the dominant in cases where the target (presumably synchrotron) photons are produced co-spatially with the high-energy radiation. Hence, polarized high-energy emission produced co-spatially with polarized target (synchrotron) photons is expected to be subject to smaller $\gamma\gamma$ absorption than in the (commonly considered) case of unpolarized photons.

Interestingly, the effect described above will lead to an increase in the degree of polarization with increasing photon energy, at the transition from optically thin to optically thick (to $\gamma\gamma$ absorption) photon energies. Figure 3 illustrates this feature. The bottom panel shows the spectral break resulting from internal $\gamma\gamma$ absorption, while the top panel shows the degree of polarization as a function of photon energy across the spectral break. The resulting effect is very small and most likely below the capabilities of any γ -ray polarimeters in the near future. However,

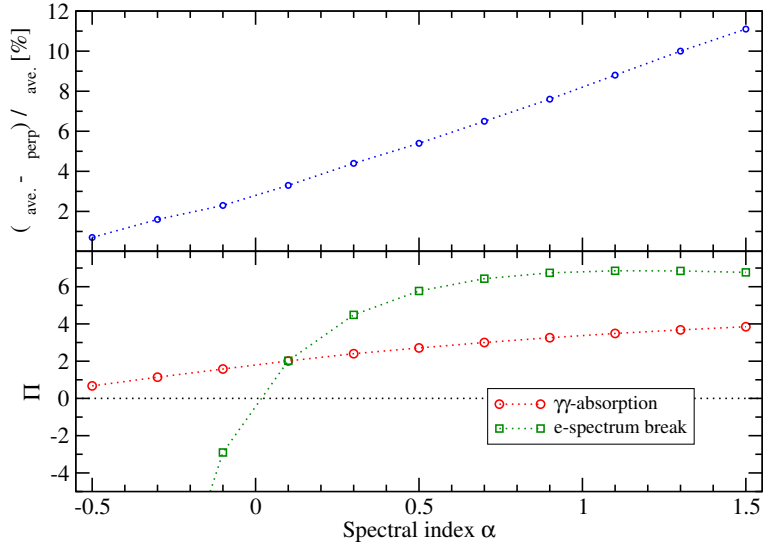


Figure 4: *Upper panel:* Ratio of unpolarized (i.e., average) to polarized (perpendicular) $\gamma\gamma$ opacity as a function of spectral index α . *Lower panel:* Change of the degree of polarization Π across the spectral break, as a function of spectral index α , expected for a break caused by polarization-dependent $\gamma\gamma$ -absorption (circles) and for a break caused by a break in the underlying electron spectrum (squares).

this result may be contrasted with the expected change of polarization in the case that a spectral break reflects a spectral break in the underlying electron distribution (i.e., a change of the value of $\Pi_{\max} = (p + 1)/(p + 7/3)$, where p is the spectral index of the electron distribution). This comparison is shown in the lower panel of Figure 4 for a range of spectral indices α of the target photon field (energy flux $F_\nu \propto \nu^{-\alpha}$), illustrating that an essentially unchanged degree of polarization across a spectral break provides evidence for the spectral break being caused by internal $\gamma\gamma$ absorption rather than a break in the underlying electron distribution.

The upper panel of Figure 4 shows the percentage error incurred when calculating the internal $\gamma\gamma$ opacity assuming unpolarized emission, in a maximally polarized target photon field of spectral index α . It illustrates that this error is realistically $\lesssim 10\%$. Thus, given the approximations entering Doppler factor estimates as presented in [2, 13], the impact of the polarization-dependence of $\gamma\gamma$ absorption on such estimates may be considered negligible.

4. Optical Polarization-Angle Swings

In several instances (e.g., [17, 18, 1]), γ -ray and multi-wavelength flaring activity of blazars has been observed to be accompanied by large-angle ($\geq 180^\circ$) swings of the optical polarization angle. Such events have been argued to be a signature of helical magnetic field structures (e.g., [16, 20]) and attributed to helical trajectories of emission regions [1]. Alternatively, Marscher [19] proposed a Turbulent Extreme Multi-Zone model of stochastic activation of small-scale regions with randomly oriented magnetic fields, which may lead to the often observed random-walk like polarization-angle swings, but occasionally also lead to organized large-angle swings.

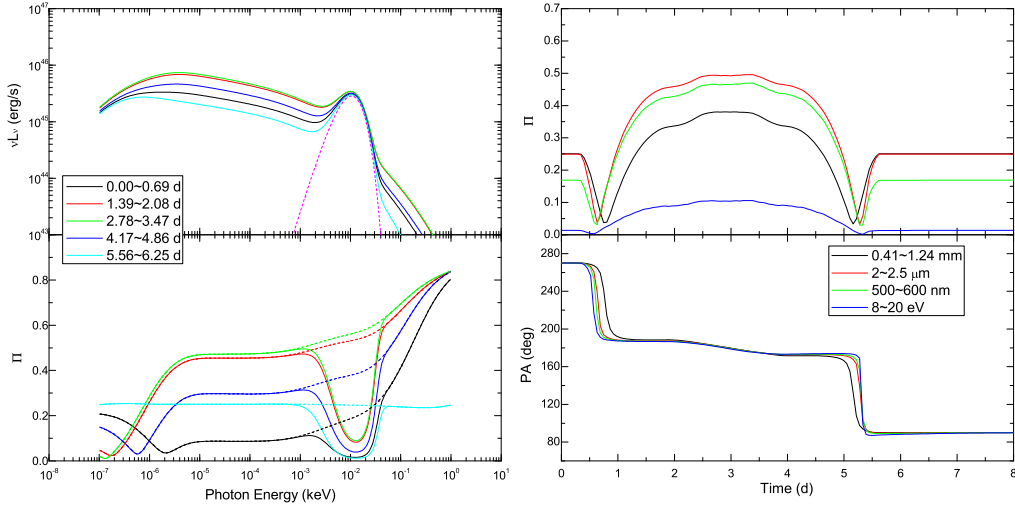


Figure 5: Photon-energy and time-dependent polarization signatures for a flaring scenario characterized by a change of the direction and strength of the magnetic field for the quasar PKS 1510-089. *Top left:* Synchrotron SEDs including the external photon field contribution, at approximately the beginning of the flare (black), immediately before the peak (red), around the peak time (green), shortly after the peak (dark blue) and back in equilibrium (light blue). The dashed line represents the external photon field contribution. *Top right:* Multiwavelength light curves including the external photon field contribution, at radio (black), infrared (red), optical V band (green), and UV (blue) frequencies. *Bottom left:* Synchrotron polarization fraction as a function of photon energy, including the external photon field, for the same time bins as in the top left panel. The dashed lines represent the polarization percentage of only the synchrotron emission (without accretion disk contamination). *Bottom right:* Polarization percentage vs. time, and PA vs. time for the same photon energy bins as in the top right panel.

Zhang et al. [25] have demonstrated that no helical motions or other non-symmetric jet features are required to reproduce correlated polarization-angle swings with multi-wavelength flaring activity, when carefully considering all light-travel-time effects in a straight jet pervaded by a helical magnetic field. They have shown that a shock-in-jet model, in which a mildly relativistic shock traverses an active region, embedded in a helical magnetic field, leads to increased particle acceleration and magnetic-field amplification, naturally produces polarization-angle swings associated with γ -ray (and multi-wavelength) flares. Their simulations are based on Fokker-Planck / Monte-Carlo simulations of electron dynamics and radiation transfer using the code of Chen et al. [11, 12], whose resulting space- and time-dependent electron distributions are then used in a separate polarization-dependent ray tracing code [25] to predict the time- and photon-energy dependent polarization signatures.

Figure 5 illustrates an example of the results for a case study based on the observed SEDs and light curves of the quasar PKS 1510-089. In the simplest case of a length of the active region much larger than the width of the jet, this results in a succession of two step-like 90° polarization-angle

rotations, associated with drastic changes in the degree of polarization at various photon energies. Such step-like rotations have, in fact, been observed in a few cases (e.g., [15]).

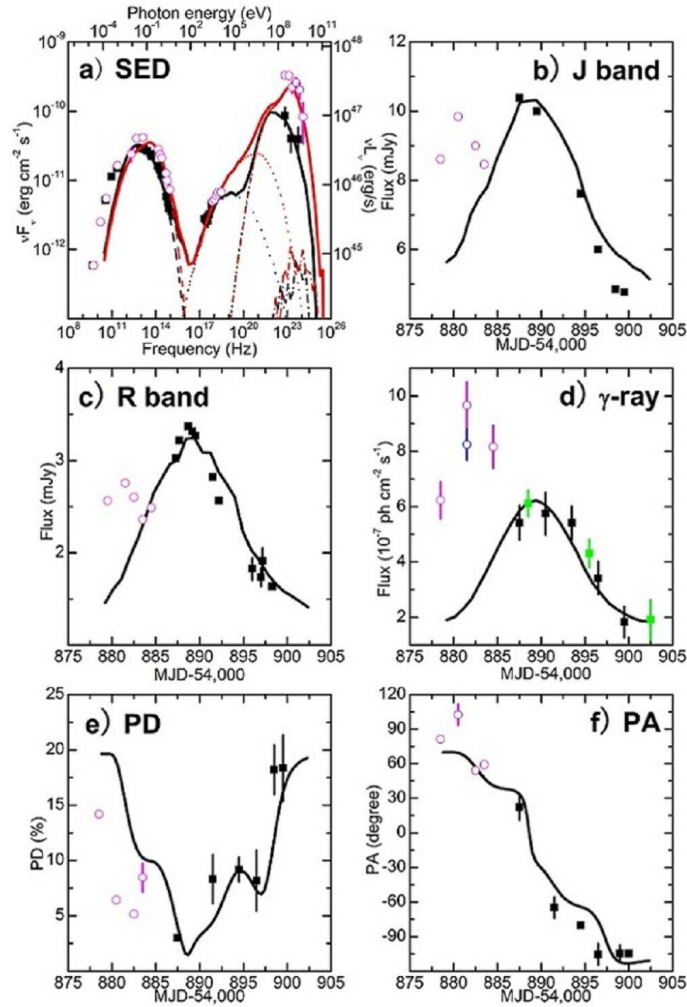


Figure 6: Data and model fits to multi-wavelength SEDs, light curves and polarization signatures during the second flare of 3C279 in 2009. Data are from [1, 14]. a) SEDs. Black squares are from Period E in [14] (MJD 54897 – 54900), corresponding to the end of the second flare. The black curve is the model SED from the simulation at the same period; the red curve is the simulated SED at the peak of the flare. Hollow magenta circles are from Period D (MJD 54880 – 54885), corresponding to the end of the first flare. b, c, d) J and R Band and Fermi-LAT γ -ray light curves; the black curves are the simulated light curves. e, f) Polarization Degree (PD) and Polarization Angle (PA) vs. time: black squares and hollow magenta circles are from the second and the first flare, respectively; curves are the simulated polarization signatures.

However, different geometrical parameters may be chosen to reproduce smoother rotations. As a specific application of this model, Zhang et al. [26] modelled time-dependent SEDs, multi-wavelength light curves, and time-dependent polarization degrees and polarization angles at various photon energies as observed in the prominent polarization-angle swing event in the quasar 3C279 [1, 14] in 2009. As the γ -ray and optical flares around the polarization-angle swings seem to be composed of two separate (possibly independent) sub-flares, their modeling focused on the

second sub-flare. The results are illustrated in Figure 6. Details of the model parameters may be found in [26]. The most important requirement for reproducing the γ -ray flaring event without significant flaring activity in the optical (synchrotron) emission, in tandem with the observed changes in the polarization signatures, is that the magnetic field needs to decrease by about 25 % from the pre-flare to the flare state. This reduction in the magnetic field needs to be accompanied by the injection (impulsive acceleration) of additional relativistic electrons in the emission region. Thus, this simultaneous fitting of SEDs, light curves and polarization signatures, requires a transfer of magnetic energy into particle energy, possibly hinting to magnetic reconnection as the driving mechanism of such multi-wavelength flaring activity.

References

- [1] Abdo, A. A., et al., 2010, *Nature*, 463, 919
- [2] Baring, M. G., 1993, *ApJ*, 418, 391
- [3] Blandford, R. D., & Znajek, R. L., 1977, *MNRAS*, 179, 433
- [4] Blandford, R. D., & Pyne, D. G., 1982, *MNRAS*, 199, 883
- [5] Böttcher, M., Reimer, A., Sweeney, K., and Prakash, A., 2013, *ApJ*, 768, 54
- [6] Böttcher, M., 2014, *ApJ*, 795, 35
- [7] Bonometto, S., Cazzola, P., & Saggion, A., 1970, *A&A*, 7, 292
- [8] Bonometto, S., & Saggion, A., 1973, *A&A*, 23, 9
- [9] Breit, G., & Wheeler, J. A., 1934, *Phys. Rev.*, 46, 1087
- [10] Bühler, R., et al., 2010, Talk at SCINEGHE 2010 Trieste, http://www.rolfbuehler.net/index_talks.html
- [11] Chen, X., Fossati, G., Liang, E. P., & Böttcher, M., 2011, *MNRAS*, 416, 2368
- [12] Chen, X., Fossati, G., Böttcher, M., & Liang, E., 2012, *MNRAS*, 424, 789
- [13] Dondi, L., & Ghisellini, G., 1995, *MNRAS*, 273, 583
- [14] Hayashida, M., et al., 2012, *ApJ*, 754, 114
- [15] Ikejiri, Y., et al., 2011, *PASJ*, 63, 639
- [16] Lyutikov, M., Pariev, V. I., & Gabuzda, D. C., 2005, *MNRAS*, 360, 869
- [17] Marscher, A. P., et al., 2008, *Nature*, 452, 966
- [18] Marscher, A. P., et al., 2010, *ApJ*, 710, L126
- [19] Marscher, A. P., 2014, *ApJ*, 780, 87
- [20] Pushkarev, A. B., Gabuzda, D. C., Vetukhnovskaya, Y. N., & Yakimov, V. E., 2005, *MNRAS*, 356, 859
- [21] Rybicki, G. B., & Lightman, A. P., 1985, *Radiative Processes in Astrophysics* (New York: Wiley)
- [22] Wu, X., et al., 2014, in *Proc. of the SPIE*, Vol. 9144, id. 91440F (arXiv:1407.0710)
- [23] Zdziarski, A. A., & Böttcher, M., 2015, *MNRAS*, 450, 21

- [24] Zhang, H., & Böttcher, M., 2013, ApJ, 774, 18
- [25] Zhang, H., Chen, X., & Böttcher, M., 2014, ApJ, 789, 66
- [26] Zhang, H., Chen, X., Böttcher, M., Guo, F., & Li, H., 2015, ApJ, 804, 58